International Food Research Journal 28(1): 102 - 109 (February 2021)
Journal homepage: *http://www.ifrj.upm.edu.my*

Synthesis of ZnO nanoparticles using *Theobroma cacao* L. pod husks, and their antibacterial activities against foodborne pathogens

Sarillana, Z. C., Fundador, E. O. and *Fundador, N. G.

Department of Food Science and Chemistry, College of Science and Mathematics, University of the Philippines Mindanao, Mintal, Tugbok District, Davao City 8022, Philippines

Article history

Received: 12 May 2020
Received in revised form: 16 July 2020
Accepted: 22 September 2020

Keywords

antimicrobial, biosynthesis, Theobroma cacao L. pod husk, ZnONPs

Abstract

Zinc oxide nanoparticles (ZnONPs) with antimicrobial properties have potential applications in the food industry. In the present work, the biosynthesis of ZnONPs was carried out using *Theobroma cacao* L. pod husk extract. UV-Vis spectroscopy confirmed NP formation by the presence of a peak in the range of 390 - 360 nm. Different parameters affecting the biosynthesis were assessed. A temperature of 28°C and pH of 7 were the best conditions for the formation of small-sized NPs. The antibacterial activity of ZnONPs was evaluated using the resazurin microtiter assay. The minimum inhibitory concentrations of ZnONPs for *Escherichia coli* and *Staphylococcus aureus* were 6.25 and 12.5 µg/mL, respectively. ZnONPs were more potent than chloramphenicol, suggesting that they are effective against chloramphenicol-resistant bacteria. Based on scanning electron microscopy and transmission electron microscopy, the ZnONPs were irregular in shape, with an average size of 81 nm. The results of the present work provide a simple, cost-effective, and eco-friendly method for the large-scale production of ZnONPs. Moreover, the study highlights the potential of ZnONPs as an antimicrobial agent that can be applied to food packaging systems, textiles, and medical devices.

Introduction

Pathogenic microorganisms in food pose a considerable problem in the food industry, and threaten the health of consumers. Therefore, their growth must be critically controlled and prevented throughout the production. Each year, the consumption of unsafe food products leads to approximately 600 million cases of foodborne illnesses (WHO, 2019). In the Philippines, food prepared by food service establishments is the leading cause of foodborne disease outbreaks (Azanza *et al.,* 2019). Common antimicrobial agents (e.g., citric acid and sodium benzoate) have been incorporated in products to help address this food safety issue. However, several strains of pathogenic bacteria have already developed resistance against these agents. Hence, food industries must search for new antimicrobial agents that can minimise the risks of pathogenic microorganisms.

Nanotechnology involves the manufacture of materials and devices conducted in nanoscale ranging from 1 to 100 nm (Sweet *et al.,* 2012). In food science, nanoparticles (NPs) have been applied to enhance the integrity of packaging systems and extending the shelf life of food products (Singh *et al.,* 2017). Metal oxide NPs, such as zinc oxide NPs (ZnONPs), have been reported to have antibacterial potential (Rasmussen *et al.,* 2010). The toxic mechanism of ZnONPs could be through the release of Zn^{2+} ions, generation of Reactive Oxygen Species (ROS), or direct interaction of the NPs, which results in mechanical damage of the cell (Zhang *et al.,* 2016). Once exposed to a microbial cell, ZnONPs may disrupt the cell's proton motive force, distort enzyme active sites, inhibit efflux pumps, or induce stress through ROS (Agarwal *et al.,* 2018). ZnONPs have a white appearance, UV light-blocking properties, and are generally recognised as safe (GRAS) by the United States Food and Drug Administration (Espitia *et al.,* 2016).

Different approaches are employed in the preparation of ZnONPs. Polyol synthesis involves the use of multivalent alcohol (e.g., glycol) that serves as a solvent and reducing agent for metallic precursor (Mahamuni *et al.,* 2019). The physical method makes use of the high-energy ball milling process to reduce the size of ZnO to a nanoscale (Reddy *et al.,* 2019). Although these conventional methods have been effective in the preparation of NPs, the pollution caused by the chemicals and high energy requirement pose a problem to both humans and the environment (He *et al.,* 2016). On the other hand, the biological method, which makes use of plant extracts, is a simple,

*Corresponding author.
Email: nvfundador@up.edu.ph

DOI:
https://doi.org/10.47836/ifrj.28.1.10

cost-effective, and eco-friendly alternative for the synthesis of ZnONPs (Vijayakumar *et al.,* 2018). Plant parts such as leaves and flowers have been utilised for the synthesis of ZnONPs (Abbasi *et al.,* 2019; Hameed *et al.,* 2019; Lakshmeesha *et al.,* 2019; Seifunnisha and Shanthi, 2020). The presence of phytochemicals (e.g., phenolic compounds, vitamins, and terpenoids) in plants act as capping agents for NP synthesis (Agarwal *et al.,* 2017).

Theobroma cacao L. is an evergreen tree in the family Malvaceae. This high-value crop is widely grown in the Philippines and other tropical countries for the production of cacao beans. Cacao farms generate tons of cacao pod husks which are often discarded as waste. However, these pod husks contain different phenolic compounds such as stilbenoids, terpenoids, and flavonoids (Karim *et al.,* 2014) making them suitable for the preparation of NPs. In the present work, we present a facile and eco-friendly method for synthesising ZnONPs using cacao pod husk. The resulting ZnONPs were also assessed for their antibacterial potential.

Materials and methods

Plant material preparation

Theobroma cacao L. pod husks were procured from a small farm at Barangay Saloy, Calinan District, Davao City, Philippines. Plant parts (fruit, leaves, stems, and flowers) were also sent to the Bureau of Plant Industry - Davao National Crop Research, Development and Production Support Centre, Davao City for plant identification. The pod husks were washed with tap water to remove adhering foreign materials. The pod husks were then cut into pieces, and dried using Christ Alpha 1-4 LD Plus freeze dryer at -50°C for 48 h. The freeze-dried cacao pod husks were ground and stored at -70°C until further use.

Preparation of Theobroma cacao L. pod husk (TCPH) extract

The extraction of TCPH was performed following the method of Das *et al.* (2014) with some modifications. The TCPH powder was mixed with 96% ethanol in a 1:10 powder-solvent ratio. The resulting mixture was placed in a shaking incubator with a constant shaking of 100 rpm, 30°C for 72 h followed by filtration. The extract was concentrated using a Yamato RE 200 rotary evaporator until only 50% of the initial volume remained. The residue was collected and stored in a dark bottle at -20°C until further use. For total phenolic content (TPC) and 1,1-diphenyl-2-picrylhydrazyl (DPPH) free radical scavenging assays, extracts were further dried using a freeze dryer.

TPC assay

The Folin-Ciocalteu method was performed following the procedure described by Benabdallah *et al.* (2016). TCPH extract (0.5 mL) with a concentration of 1 mg/mL was mixed with 2 mL Folin-Ciocalteu reagent. After 5 min, 2.5 mL of 7.5% Na_2CO_3 was added to the mixture, which was then incubated for 90 min at room temperature. The absorbance was measured at 760 nm using a Shimadzu UV-1700 UV-Vis spectrophotometer. Gallic acid solutions (0, 50, 100, 150, 200, and 500 µg/mL) were used as standards. Results were expressed as milligrams of gallic acid equivalents per milligram of extract (mg GAE/mg extract).

DPPH free radical scavenging assay

The antioxidant activity of the TCPH extract was determined using the DPPH assay protocol described by Das *et al.* (2014). In a 96-well plate, 20 µL of the TCPH extract with different concentrations (0.8, 0.4, 0.2, 0.1, 0.05, 0.025, 0.0125, and 0.00625 mg/mL) was prepared by two-fold serial dilution. To each well, 180 µL of 0.1 mM DPPH (1,1-diphenyl-2-picrylhydrazyl) solution was added. The plate was incubated in the dark for 30 min. The absorbance of the sample was measured at 520 nm using a PerkinElmer Victor X4 Multimode Plate Reader. Each plate had the following set of controls: a column with ascorbic acid as the positive control and a column with H_2O as the negative control. The DPPH scavenging activity was calculated using Eq. 1.

$$\% \text{ DPPH scavenging activity} = \frac{\text{Abs control - Abs sample}}{\text{Abs control}} \times 100 \quad \text{(Eq. 1)}$$

The IC_{50} was obtained by plotting the concentration of the extract against its respective % DPPH scavenging activity.

Biosynthesis of ZnONPs

The biosynthesis of ZnONPs was performed following the method described by Jafarirad *et al.* (2016) with some modifications. Ten millilitres of TCPH extract were mixed with 40 mL of 50 mM $Zn(CH_3COO)_2$. The mixture was stirred and incubated in a shaker at 28°C for 1 h. After shaking, the pH condition was adjusted to pH 7 using 0.2 M NaOH, and re-incubated in a shaker at 28°C for 1 h. The mixture was then centrifuged at 4°C and 4,500 rpm for 10 min. The precipitate was washed with ethanol followed with deionised water. After this, the

precipitate was heat-treated in a furnace for 5 h at 400°C. The formation of ZnONPs was confirmed by reading the absorption spectra of the powder in the solution from 800 - 200 nm using the Shimadzu UV-1700 UV-Vis spectrophotometer.

For the optimisation study, the pH (7, 8, and 9) and temperature (28, 45, 60, and 80°C) of the reaction were varied.

Antimicrobial test

The antimicrobial activity of the ZnONPs was tested against *Staphylococcus aureus* (BIOTECH 1582) and *Escherichia coli* (BIOTECH 1634) using the Resazurin Microtiter Test Assay (REMA) as described by Sarker *et al.* (2007). In a 96-well plate, 100 µL of ZnONPs with varying concentrations (100, 50, 25, 12.5, 6.25, 3.125, 1.5625, and 0.78125 µg/mL) were prepared by two-fold serial dilution. To each well, 10 µL 0.02% resazurin solution was added, followed by 10 µL of the bacterial suspension (10^8 CFU/mL). Each plate had the following set of controls: columns with chloramphenicol (HiMedia, India) as the positive control, columns without the microbial suspension as sterility control, and columns without ZnONPs as the negative control. The plate was then placed in an incubator for 18 h at 37°C. A change in colour from blue to pink or violet indicates the presence of microbial growth. The relative fluorescence unit (RFU) in each well was measured using a 530 nm excitation filter and a 590 nm emission filter (PerkinElmer Victor X4 Multimode Plate Reader). The percentage inhibition was calculated using Eq. 2

$$\% \text{ inhibition} = \left[1 - \left(\frac{\text{RFU sample} - \text{RFU sterility control}}{\text{RFU negative control} - \text{RFU sterility control}}\right)\right] \times 100 \quad \text{(Eq. 2)}$$

The minimum inhibitory concentration (MIC) is defined as the lowest concentration of ZnONPs, where at least 80% of bacterial growth was inhibited (Sharma *et al.,* 2014).

Field emission - scanning electron microscopy (FE-SEM) and transmission electron microscopy (TEM)

ZnONP samples were sent to the Department of Mining, Metallurgical and Materials Engineering at the University of the Philippines Diliman for field emission - scanning electron microscopy (FE-SEM) analysis. Samples were also sent to the Department of Science and Technology, Industrial Technology Development Institute (DOST-ITDI) for transmission electron microscopy (TEM) analysis.

Photocatalytic activity

One millilitre of the ZnONP solution (5 mg/mL) was mixed with 4 mL of methylene blue solution (0.015 mM). The solution was placed under black light exposure for 45 min. The absorbance was read at 668 nm, and the % colour change was then calculated using Eq. 3.

$$\% \text{ Colour change} = \frac{\text{Initial Abs} - \text{Final Abs}}{\text{Initial Abs}} \times 100 \quad \text{(Eq. 3)}$$

Statistical analysis

Triplicate experiments were conducted. One-way analysis of variance (ANOVA) and Tukey's HSD test at $p < 0.05$ level of significance determined the significant difference between treatments.

Results and discussion

Characterisation of the TCPH extract

The TPC of the TCPH extract was 0.145 ± 0.010 mg GAE/mg TCPH extract. DPPH free radical assay resulted in an IC_{50} of 0.175 ± 0.003 mg/mL as shown in Figure 1. According to Karim *et al.* (2014), TCPH contains phenolic compounds such as stilbenoids, terpenoids, and flavonoids. The presence of these compounds may have significantly contributed to the TPC value of the TCPH extract as well as its DPPH scavenging activity.

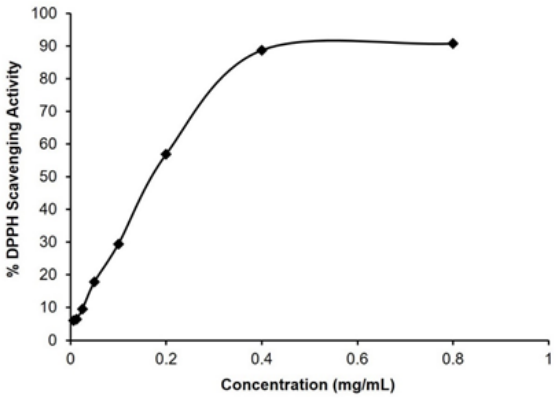

Figure 1. Percentage DPPH scavenging activities of different concentrations of *Theobroma cacao* L. pod husk extract (IC_{50} = 0.175 ± 0.003 mg/mL).

Biosynthesis of zinc oxide nanoparticles (ZnONPs)

The biosynthesis of ZnONPs was carried out in the presence of TCPH extract. The NP formation was confirmed by the presence of a peak with λ_{max} value in the range of 390 - 360 nm (Zare *et al.,* 2017). The position of the absorption peak is related to the size of the NP. As the NPs increase in size, the absorption peak shifts to a longer wavelength (red shift). However, the absorption peak shifts to a shorter wavelength (blue shift) as the size of the NPs decreases

(Umadevi *et al.,* 2012).

It is noteworthy that a precipitate was formed at pH 7, 8, and 9, even without the help of plant extracts. However, the absence of absorbance peaks indicates that the ZnO formed were not NPs. It is believed that Zn^{2+} precipitated as $Zn(OH)_2$, and then converted to ZnO after heating. This contrasts the claims of other studies, which stated that plant extracts reduce Zn^{2+} to elemental Zn (Jamdagni *et al.,* 2018; Ramanarayanan *et al.,* 2018). The compounds present in the plant extracts may serve as capping agents to control the growth and aggregation of nanoparticles (Mittal *et al.,* 2017). This claim is supported by the analysis done by research groups confirming the presence of phenolic compounds on the surface of the NP (Zhao *et al.,* 2018; Mirza *et al.,* 2019; Pillai *et al.,* 2020).

The ability of the TCPH extract to aid in the synthesis of ZnONPs may be influenced by factors such as temperature and pH. Thus, an optimisation study was conducted to determine the conditions that would lead to the production of smaller-sized NPs.

Effect of temperature

Figure 2A shows that the λ_{max} of ZnONPs synthesised at 28, 45, 60, and 80°C did not vary significantly. Statistical analysis shows that the values among peaks were not significantly different ($p < 0.05$). A similar finding was reported by Jamdagni *et al.* (2018). This suggests that the formation of ZnONPs is not temperature-dependent. Thus, 28°C was used in the subsequent experiment

Effect of pH

The λ_{max} values for ZnONPs synthesised at pH 7, 8, and 9 were 372, 383, and 391 nm, respectively. A broad and almost undetectable absorption peak was observed at pH 9 (Figure 2B). The redshift and broadening at higher pH could be due to the aggregation of the NPs. In another study, ZnONPs produced using seaweed extract showed no absorption peak at pH 9 and 10 (Nagarajan and Kuppusamy, 2013). At higher pH, some phenolics (Friedman and Jürgens, 2000) become unstable. Therefore, the ability of these biomolecules to act as capping agents might be compromised at higher pH values. This would result in larger-sized NPs. Statistical analysis shows that there was a significant increase in the λ_{max} values of ZnONP peaks with increasing pH ($p < 0.05$). Indeed, high pH would result in larger-sized NPs.

Based on the absorption peaks, the smallest NP size was obtained at pH 7. According to Jamdagni *et al.* (2018), smaller-sized NPs are preferred due to their high surface area to volume ratio and better

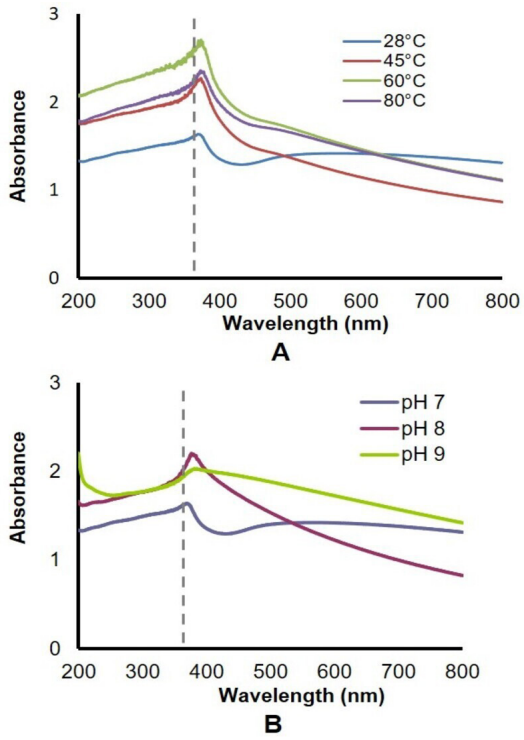

Figure 2. UV-Vis absorption spectra of ZnONPs synthesised using *Theobroma cacao* L. pod husk extract at varying (A) temperatures, and (B) pH's.

toxicity against microorganisms. Hence, the optimum pH value for ZnONP synthesis was at 7.

Antimicrobial test

The antimicrobial potential of ZnONPs was tested on two common foodborne pathogens, *E. coli* and *S. aureus*. As shown in Table 1, the MIC of *S. aureus* (12.5 µg/mL) was higher as compared to *E. coli* (6.25 µg/mL). This implies that ZnONPs were more potent against *E. coli* than *S. aureus*. Gram-negative bacteria, such as *E. coli*, have lipopolysaccharides and peptidoglycans on their cell wall. This arrangement of layers may facilitate the entrance of ROS, ions, and small ZnONPs into the cell (Slavin *et al.,* 2017). In the case of *S. aureus*, the thick peptidoglycan layer of the Gram-positive bacteria may have served as a protective layer against ZnONPs (Slavin *et al.,* 2017). Thus, a higher concentration of ZnONPs was needed to inhibit *S. aureus* as compared to *E. coli*.

Table 1. Minimum inhibitory concentrations (MIC) and percent inhibition of ZnONPs and chloramphenicol for bacteria as determined using REMA.

Test microorganism	MIC (µg/mL)	% Inhibition	
		ZnONPs	Chloramphenicol
E. coli	6.25 ± 0.00	93.229 ± 2.24[a]	65.898 ± 2.92[b]
S. aureus	12.5 ± 0.00	87.489 ± 2.10[a]	66.479 ± 2.29[b]

Values are mean of triplicate ($n = 3$) ± standard deviation (SD). Means with different superscript in a row are significantly different ($p < 0.05$).

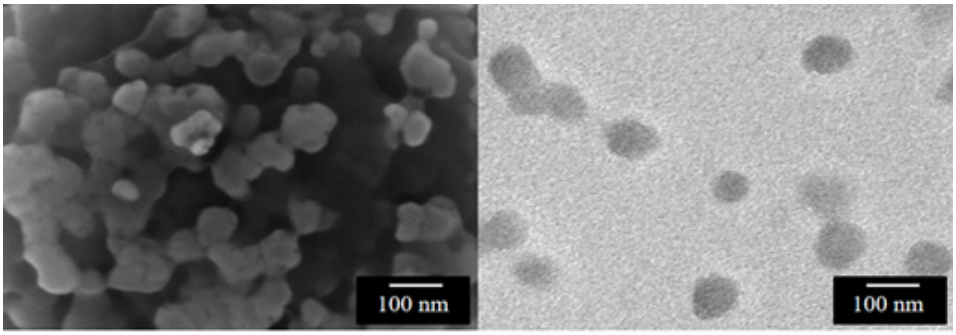

Figure 3. (A) Field emission - scanning electron, and (B) transmission electron micrographs of ZnONPs synthesised at pH 7 and 28°C.

Furthermore, the present work also compared the percentage of inhibition of ZnONPs against chloramphenicol. Results of the fluorometric readings suggest that ZnONPs exhibited higher inhibition than chloramphenicol against both bacteria. The differences in their mechanism of action can explain these results. According to Zhang *et al.* (2016), the toxic effects of ZnONPs could be due to the release of Zn^{2+} ions into the cell, generation of ROS, or the direct interaction of the ZnONPs. This results in the damage of the bacterial cell and eventually, cell death. Chloramphenicol, on the other hand, is a broad-spectrum antibiotic that inhibits the elongation of protein chains (Das and Patra, 2017). Based on the findings, ZnONP is more potent than chloramphenicol. The bacterial strains used may have developed resistance against chloramphenicol. The mutation or modification of the target site among bacterial cells may be the reason for the emerging antimicrobial resistance against chloramphenicol (Andrews, 2001).

FE-SEM and TEM analyses

The FE-SEM and TEM images of the ZnONPs are shown in Figure 3. Under FE-SEM, the produced ZnONPs looked irregular in shape. The TEM images also revealed that the average size of the ZnONPs was 81 nm. Bagabas *et al.* (2013) produced similar ZnONPs, wherein they obtained irregular-shaped NPs with an average size of 40 nm. According to a study by Penders *et al.* (2017), NPs with irregular shapes, spikes, and star-like structures have more antibacterial effects than those without. This behaviour may be explained by their high surface area, which provides greater contact points for microbial growth inhibition.

Photocatalytic activity

Metal oxides, such as ZnONPs, have been reported as good photocatalysts in degrading pollutants such as organic dyes. In the present work, the synthesised ZnONPs were able to degrade methylene blue when exposed to black light. The degradation of methylene blue was manifested by the reduction of the intensity of the blue colour. A 26.35% colour reduction of methylene blue was observed after 45 min of exposure to black light. The photocatalytic activity exhibited by ZnONPs is due to the production of negative-electron (e^-) and positive-hole (h^+) pairs in the presence of ultraviolet light or visible light irradiation. During the photocatalytic degradation process, the electron-hole pair reacts with the O_2 on the surface of ZnONPs as well as the surrounding H_2O to generate hydroxyl radicals which are responsible for the degradation of organic contaminants into their non-toxic end forms (Chen *et al.,* 2017).

Conclusion

ZnONPs were synthesised using the TCPH extract. The phenolic compounds present in the extract served as a capping agent to control the formation of the NPs, as suggested in previous studies. Reaction conditions set at 28°C and pH 7 produced ZnONPs with an irregular shape, and an average size of 81 nm. The antimicrobial test revealed that the ZnONPs were more potent than chloramphenicol. The findings of the present work open the possibility of exploring underutilised plant materials to provide a cost-effective and eco-friendly approach for the synthesis of ZnONPs. Cytotoxicity tests are recommended to evaluate the toxicity of ZnONPs in cells. Future studies on the application of ZnONPs in food packaging, cosmetics, textiles, and therapeutic drugs can also be explored.

Acknowledgement

The authors would like to express their gratitude to the University of the Philippines System

Enhanced Creative Work and Research Grant (UP ECWRG 2018-1-016) for financially supporting the present work, and Dr. Joel Hassan Tolentino of the UP Mindanao for the use of laboratory equipment.

References

Abbasi, B. A., Iqbal, J., Ahmad, R., Zia, L., Kanwal, S., Mahmood, T., ... and Chen, J.-T. 2019. Bioactivities of *Geranium wallichianum* leaf extracts conjugated with zinc oxide nanoparticles. Biomolecules 10(1): article no. 38.

Agarwal, H., Venkat Kumar, S. and Rajeshkumar, S. 2017. A review on green synthesis of zinc oxide nanoparticles - an eco-friendly approach. Resource-Efficient Technologies 3(4): 406-413.

Agarwal, H., Menon, S., Venkat Kumar, S. and Rajeshkumar, S. 2018. Mechanistic study on antibacterial action of zinc oxide nanoparticles synthesized using green route. Chemico-Biological Interactions 286: 60-70.

Andrews, J. M. 2001. Determination of minimum inhibitory concentrations. Journal of Antimicrobial Chemotherapy 48(Suppl. 1): 5-16.

Azanza, M. P. V., Membrebe, B. N. Q., Sanchez, R. G. R., Estilo, E. E. C., Dollete, U. G. M., Feliciano, R. J. and Garcia, N. K. A. 2019. Foodborne disease outbreaks in the Philippines (2005-2018). Philippine Journal of Science 148(2): 323-342.

Bagabas, A., Alshammari, A., Aboud, M. F. A. and Kosslick, H. 2013. Room-temperature synthesis of zinc oxide nanoparticles in different media and their application in cyanide photodegradation. Nanoscale Research Letters 8: article no. 516.

Benabdallah, A., Rahmoune, C., Boumendjel, M., Aissi, O. and Messaoud, C. 2016. Total phenolic content and antioxidant activity of six wild *Mentha* species (Lamiaceae) from northeast of Algeria. Asian Pacific Journal of Tropical Biomedicine 6(9): 760-766.

Chen, X., Wu, Z., Liu, D. and Gao, Z. 2017. Preparation of ZnO photocatalyst for the efficient and rapid photocatalytic degradation of azo dyes. Nanoscale Research Letters 12(1): article no. 143.

Das, B. and Patra, S. 2017. Antimicrobials: meeting the challenges of antibiotic resistance through nanotechnology. In Ficai, A. and Grumezescu, A. M. (eds). Nanostructures for Antimicrobial Therapy, p. 1-22. United States: Elsevier.

Das, N., Islam, M., Jahan, N., Islam, M. S., Khan, A., Islam, M. R. and Parvin, M. 2014. Antioxidant activities of ethanol extracts and fractions of *Crescentia cujete* leaves and stem bark and the involvement of phenolic compounds. BMC Complementary and Alternative Medicine 14: article no. 45.

Espitia, P. J. P., Otoni, C. G. and Soares, N. F. F. 2016. Zinc oxide nanoparticles for food packaging applications. In Barros-Velázquez, J. (ed). Antimicrobial Food Packaging, p. 425-431. United States: Academic Press.

Friedman, M. and Jürgens, H. S. 2000. Effect of pH on the stability of plant phenolic compounds. Journal of Agricultural and Food Chemistry 48(6): 2101-2110.

Hameed, S., Iqbal, J., Ali, M., Khalil, A. T., Abbasi, B. A., Numan, M. and Shinwari, Z. K. 2019. Green synthesis of zinc nanoparticles through plant extracts: establishing a novel era in cancer theranostics. Materials Research Express 6(10): article ID 102005.

He, Y., Du, Z., Ma, S., Cheng, S., Jiang, S., Liu, Y., ... and Zheng, X. 2016. Biosynthesis, antibacterial activity and anticancer effects against prostate cancer (PC-3) cells of silver nanoparticles using *Dimocarpus longan* Lour. peel extract. Nanoscale Research Letters 11(1): article no. 300.

Jafarirad, S., Mehrabi, M., Divband, B. and Kosari-Nasab, M. 2016. Biofabrication of zinc oxide nanoparticles using fruit extract of *Rosa canina* and their toxic potential against bacteria: a mechanistic approach. Materials Science and Engineering C - Materials for Biological Applications 59: 296-302.

Jamdagni, P., Khatri, P. and Rana, J. S. 2018. Green synthesis of zinc oxide nanoparticles using flower extract of *Nyctanthes arbor-tristis* and their antifungal activity. Journal of King Saud University - Science 30(2): 168-175.

Karim, A. A., Azlan, A., Ismail, A., Hashim, P. and Abdullah, N. A. 2014. Antioxidant properties of cacao pods and shells. Malaysian Cocoa Journal 8: 49-56.

Lakshmeesha, T. R., Kalagatur, N. K., Mudili, V., Mohan, C. D., Rangappa, S., Prasad, B. D., ... and Niranjana, S. R. 2019. Biofabrication of zinc oxide nanoparticles with *Syzygium aromaticum* flower buds extract and finding its novel application in controlling the growth and mycotoxins of *Fusarium graminearum*. Frontiers in Microbiology 10: article no. 1244.

Mahamuni, P. P., Patil, P. M., Dhanavade, M. J., Badiger, M. V., Shadija, P. G., Lokhande, A. C.

and Bohara, R. A. 2019. Synthesis and characterization of zinc oxide nanoparticles by using polyol chemistry for their antimicrobial and antibiofilm activity. Biochemistry and Biophysics Reports 17: 71-80.

Mirza, A. U., Kareem, A., Nami, S. A. A., Bhat, S. A., Mohammad, A. and Nishat, N. 2019. *Malus pumila* and *Juglen regia* plant species mediated zinc oxide nanoparticles: synthesis, spectral characterization, antioxidant and antibacterial studies. Microbial Pathogenesis 129: 233-241.

Mittal, J., Singh, A., Batra, A. and Sharma, M. M. 2017. Synthesis and characterization of silver nanoparticles and their antimicrobial efficacy. Particulate Science and Technology 35(3): 338-345.

Nagarajan, S. and Kuppusamy, K. A. 2013. Extracellular synthesis of zinc oxide nanoparticle using seaweeds of gulf of Mannar, India. Journal of Nanobiotechnology 11: article no. 39.

Penders, J., Stolzoff, M., Hickey, D. J., Andersson, M. and Webster, T. J. 2017. Shape-dependent antibacterial effects of non-cytotoxic gold nanoparticles. International Journal of Nanomedicine 12: 2457-2468.

Pillai, A. M., Sivasankarapillai, V. S., Rahdar, A., Joseph, J., Sadeghfar, F., Anuf A. R., ... and Kyzas, G. Z. 2020. Green synthesis and characterization of zinc oxide nanoparticles with antibacterial and antifungal activity. Journal of Molecular Structure 1211: article ID 128107.

Ramanarayanan, R., Bhabhina, N. M., Dharsana, M. V., Nivedita, C. V. and Sindhu, S. 2018. Green synthesis of zinc oxide nanoparticles using extract of *Averrhoa bilimbi* (L.) and their photoelectrode applications. Materials Today - Proceedings 5(8): 16472-16477.

Rasmussen, J. W., Martinez, E., Louka, P. and Wingett, D. G. 2010. Zinc oxide nanoparticles for selective destruction of tumor cells and potential for drug delivery applications. Expert Opinion on Drug Delivery 7(9): 1063-1077.

Reddy, I. N., Reddy, C. V., Sreedhar, M., Shim, J., Cho, M. and Kim, D. 2019. Effect of ball milling on optical properties and visible photocatalytic activity of Fe doped ZnO nanoparticles. Materials Science and Engineering B 240: 33-40.

Sarker, S. D., Nahar, L. and Kumarasamy, Y. 2007. Microtitre plate-based antibacterial assay incorporating resazurin as an indicator of cell growth, and its application in the *in vitro* antibacterial screening of phytochemicals. Methods 42(4): 321-324.

Seifunnisha, O. and Shanthi, J. 2020. Aloe vera mediated green synthesis of ZnO nanostructure under sol-gel method: effect of antimicrobial activity. Journal of Nano- and Electronic Physics 12(2): article ID 02041.

Sharma, S., Gelman, E., Narayan, C., Bhattacharjee, D., Achar, V., Humnabadkar, V., ... and Dinesh, N. 2014. Simple and rapid method to determine antimycobacterial potency of compounds by using autoluminescent *Mycobacterium tuberculosis*. Antimicrobial Agents and Chemotherapy 58(10): 5801-5808.

Singh, T., Shukla, S., Kumar, P., Wahla, V., Bajpai, V. K. and Rather, I. A. 2017. Application of nanotechnology in food science: perception and overview. Frontiers in Microbiology 8: article no. 1501.

Slavin, Y. N., Asnis, J., Häfeli, U. O. and Bach, H. 2017. Metal nanoparticles: understanding the mechanisms behind antibacterial activity. Journal of Nanobiotechnology 15(1): article no. 65.

Sweet, M. J., Chesser, A. and Singleton, I. 2012. Metal-based nanoparticles; size, function, and areas for advancement in applied microbiology. Advances in Applied Microbiology 80: 113-142.

Umadevi, M., Shalini, S. and Bindhu, M. R. 2012. Synthesis of silver nanoparticle using *D. carota* extract. Advances in Natural Sciences - Nanoscience and Nanotechnology 3(2): article ID 025008.

Vijayakumar, S., Mahadevan, S., Arulmozhi, P., Sriram, S. and Praseetha, P. K. 2018. Green synthesis of zinc oxide nanoparticles using *Atalantia monophylla* leaf extracts: characterization and antimicrobial analysis. Materials Science in Semiconductor Processing 82: 39-45.

World Health Organization (WHO). 2019. Food safety. Retrieved on February 24, 2020 from WHO website: www.who.int/news-room/-fact-sheets/detail/food-safety

Zare, E., Pourseyedi, S., Khatami, M. and Darezereshki, E. 2017. Simple biosynthesis of zinc oxide nanoparticles using nature's source, and its *in vitro* bio-activity. Journal of Molecular Structure 1146: 96-103.

Zhang, W., Bao, S. and Fang, T. 2016. The neglected nano-specific toxicity of ZnO nanoparticles in the yeast *Saccharomyces cerevisiae*. Scientific Reports 6: article ID 24839.

Zhao, C., Zhang, X. and Zheng, Y. 2018. Biosynthesis of polyphenols functionalized ZnO nanoparticles: characterization and their effect on human pancreatic cancer cell line. Journal of

Photochemistry and Photobiology B - Biology 183: 142-146.